New Journal of Physics
The open access journal at the forefront of physics

Deutsche Physikalische Gesellschaft DPG IOP Institute of Physics

PAPER • OPEN ACCESS

Pursuit problem with a stochastic prey that sees its chasers

To cite this article: Meng Su *et al* 2023 *New J. Phys.* **25** 023033

IOP Publishing New J. Phys. 25 (2023) 023033 https://doi.org/10.1088/1367-2630/acbc42

New Journal of Physics
The open access journal at the forefront of physics

Deutsche Physikalische Gesellschaft DPG
IOP Institute of Physics

Published in partnership with: Deutsche Physikalische Gesellschaft and the Institute of Physics

OPEN ACCESS

RECEIVED
19 October 2022

REVISED
27 January 2023

ACCEPTED FOR PUBLICATION
15 February 2023

PUBLISHED
1 March 2023

PAPER

Pursuit problem with a stochastic prey that sees its chasers

Meng Su[1,5], **Davide Bernardi**[2,5] **and Benjamin Lindner**[3,4,*]

[1] School of Mathematics and Statistics, Northwestern Polytechnical University, 710129 Xi'an, Shaanxi, People's Republic of China
[2] Center for Translational Neurophysiology of Speech and Communication, Fondazione Istituto Italiano di Tecnologia, via Fossato di Mortara 19, 44121 Ferrara, Italy
[3] Department of Physics, Humboldt Universität zu Berlin, Newtonstr 15, 12489 Berlin, Germany
[4] Bernstein Center for Computational Neuroscience, Haus 2, Philippstr 13, 10115 Berlin, Germany
[5] These authors contributed equally.
[*] Author to whom any correspondence should be addressed.

E-mail: benjamin.lindner@physik.hu-berlin.de

Keywords: chase, pursuit, stochastic, Langevin dynamics, microswimmers

Abstract

A recent stochastic pursuit model describes a pack of chasers (hounds) that actively move toward a target (hare) that undergoes pure Brownian diffusion (Bernardi and Lindner 2022 *Phys. Rev. Lett.* **128** 040601). Here, this model is extended by introducing a deterministic 'escape term', which depends on the hounds' positions. In other words, the hare can 'see' the approaching hounds and run away from them, in addition to the 'blind' random diffusion. In the case of a single chaser, the mean capture time (CT) can still be computed analytically. At weak noise, the qualitative behavior of the system depends on whether the hare's maximum running drift speed is above or below a critical value (the pursuers' speed), but not on the target's viewing range, whereas the capture statistics at strong noise is similar to those of the original model without escape term. When multiple hounds are present, the behavior of the system is surprisingly similar to the original model with purely diffusing target, because the escape terms tend to compensate each other if the prey is encircled. At weak noise levels and 'supracritical' maximum escape speed, the hare can slip through the chaser pack and lead to a very strong increase of the mean CT with respect to the blind case. This large difference is due to rare events, which are enhanced when the symmetry in the initial conditions is disrupted by some randomness. Comparing the median of the CT probability density (which reflects the typical CT) with the mean CT makes clear the contribution of rare events with exceptionally long CTs.

1. Introduction

Chase-and-escape problems are a universal phenomenon in nature and a classic problem in game theory [1–3]. There are many models and methods devoted to studying optimal pursuit or escape strategies. The seemingly simplest case of this problem, i.e. only one chaser hunting a single target, can already pose challenging mathematical problems [1–8]. Different authors have also investigated more elaborate situations in which a pack of hunters chase a single prey [9, 10], a single chaser pursues a herd of prey [11, 12], or a pack of hunters chasing multiple preys [13–21]. In models describing insect swarming behaviors, individual agents can act both as predator and preys at the same time [22]. The presence of obstacles in the environment [23] and a confined space for the pursuit [9] can give the pursuit problem an additional twist.

Several of these models incorporate also random noise elements, which is particularly relevant if predators and preys are as small as, for instance, microorganisms or the increasingly popular artificial microswimmers capable of target tracking [24–29]. Typical stochastic chase-and-pursuit models, however, are either so detailed that they can only be investigated through numerical simulations [8, 13, 14, 16, 17, 19, 20, 30, 31], or rather abstract [4, 7, 32]. Analytical results have been mostly found for the case that both predators and prey are random walkers confined to a one-dimensional space [33–35], to grids [36], or to graphs [37]. This kind of predator-prey system is, in fact, closely related to the stochastic search for a fixed

target, for which many analytical results were derived in the last years [38–49]. Some results exist for predators and preys that diffuse on a square lattice and can interact at limited range [12, 50], but analytically tractable models of active chasers pursuing a randomly moving prey are scarce. Recently, a stochastic pursuit model involving multiple chasers (hounds) with a classical pursuit strategy that hunt a single, diffusively moving prey (hare) has been suggested [51, 52], a model that permits some analytical progress for the capture-time (CT) statistics.

In one of the scenarios studied in [51], N hounds start their pursuit from an equidistant arrangement on a circle centered around the hare. The disk-shaped hare moves randomly in a two-dimensional space (like an overdamped Brownian particle), while the point-like hounds deterministically run towards the hare until any of them reaches the target's circumference. Remarkably, the randomness of the prey's motion (quantified by its diffusion coefficient) can, on average, both lengthen or shorten its survival (enlarge or diminish the mean CT) depending on the number of hounds and their running speed. From the perspective of the hunter, it is furthermore interesting to note that the energy spent on hunting the prey can be minimized at a finite number of hounds and a nonvanishing but finite value of the speed of pursuit [51]. These results may have relevance for pursuit problems in nanorobotics and for problems involving natural microswimmers.

The model considered in [51] displays strong asymmetries in two respects. The chasers can see the prey and are completely deterministic, both in their dynamics as well as in their initial position. The single prey, the hare, does not 'see' the predators and behaves completely at random. What if, however, the hare can also detect the pursuers and make some use of this knowledge to escape from the hounds? This possibility is not only obviously relevant for macroscopic systems, but also for microscopic chase-and-pursuit scenarios: chemotaxis, for instance, is used not only by predators to chase preys, but also by preys to evade predators [53, 54].

In this paper, we revisit the tractable prey-pursuit model from [51] by introducing a sensible 'evasion term' into the dynamics of the hare that reflects its information (seeing) about the pursuers. The chasers still deterministically move towards the prey, and the prey tends to run away from the chasers in addition to randomly moving. We derive analytical expressions for the mean CT for the one-chaser case in one and two spatial dimensions. We also investigate the noiseless case and derive a critical condition for divergence of the CT. For the case of several chasers, the mean CT is measured by means of stochastic simulations and inspected as a function of the noise intensity for different combinations of pursuit and escape speeds and number of hounds. We investigate the existence of a 'critical' deterministic evasion speed, above which the mean CT undergoes a dramatic increase at weak noise levels, and how this critical speed depends on the number of chasers. We briefly discuss how this picture is changed by a randomization of the initial positions of the hounds. Inspecting the full CT probability density, we find that certain effects on the mean CT rely on very rare events when the hare escapes from a pack of hounds and the capture takes an unusually long time. For these cases we also compare mean and median of the distribution of CTs.

2. Model

The system consists of N chasing hounds and one target hare that move in a d-dimensional space. In this study, we will consider the cases $d = 1$ and $d = 2$ (see figure 1 for an illustration). The chasers' velocity has constant magnitude v_0 and direction always pointing to the target's position. In the original model, the prey undergoes pure Brownian diffusion. Here, the additional term $\boldsymbol{E}$ represents a deterministic escape velocity that depends on the chasers' position. The system obeys

$$\frac{\mathrm{d}\boldsymbol{X}}{\mathrm{d}t} = \sqrt{2D}\boldsymbol{\xi}(t) + \boldsymbol{E}, \tag{1}$$

$$\frac{\mathrm{d}\boldsymbol{Y}_n}{\mathrm{d}t} = v_0 \frac{\boldsymbol{X} - \boldsymbol{Y}_n}{\|\boldsymbol{X} - \boldsymbol{Y}_n\|}, \tag{2}$$

where $\boldsymbol{X}(t)$ is the hare's position, $\boldsymbol{Y}_n(t)$ is the nth hound's position ($n = 1, \ldots, N$), v_0 is the running speed of the hounds, and $\|\cdot\|$ represents the Euclidean distance. The components of $\boldsymbol{\xi}(t)$ are independent Gaussian white noise sources with unit intensity,

$$\langle \xi_i \rangle = 0, \quad \langle \xi_i(t)\xi_j(t') \rangle = \delta_{ij}\delta(t - t'), \tag{3}$$

so that D sets the intensity of the noise process, i.e. the randomness of the prey's trajectory.

The hare's initial position is the origin of the coordinate system, while the hounds are placed at the same distance from the target, and such that they are distributed around a circle equidistantly from each other. Without loss of generality, we can set the initial distance to one, which is equivalent to measuring space in

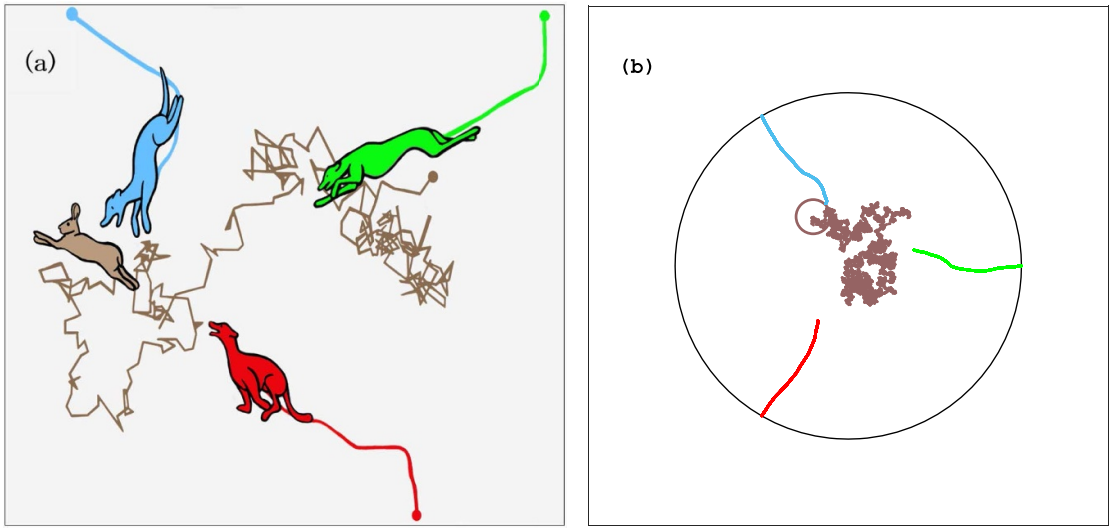

Figure 1. A pictorial illustration (a) (Reproduced with permission from Meta Laitko) and a more faithful illustration of the actual model (b). Several hounds (here $N = 3$) go after a hare (gray trajectory) which has started its random motion from the origin; hounds start at the circumference of a unit circle. The hare is captured by one of the hounds (blue trajectory).

units of the initial distance between chasers and target. The hunt terminates when the hare and any of the hounds are closer apart than a prescribed distance R, which means that the hare is described by a circle of radius R (see figure 1(b)).

Compared to the model in [51], there is a new term $\boldsymbol{E}$ modeling the hare's escape velocity v_e resulting from 'seeing' the hounds. This systematic contribution to the hare's velocity is given by a weighted sum of N terms, i.e.

$$\boldsymbol{E} = \frac{v_e}{N}\sum_{n=1}^{N} g(r_n)\,\frac{\boldsymbol{X}-\boldsymbol{Y_n}}{\|\boldsymbol{X}-\boldsymbol{Y_n}\|}. \tag{4}$$

In equation (4), the nth term of the sum is directed away from the nth chaser and is weighted according to the distance-dependent function $g(r_n)$, where $r_n = \|\boldsymbol{X}-\boldsymbol{Y_n}\|$. It is plausible that hounds further away contribute less to the escape velocity term; we choose a simple exponential decay for the weighting function:

$$g(r_n) = \exp\left[-\frac{r_n - R}{S}\right]. \tag{5}$$

Here S sets the decay rate of the weighting function from its maximum value $g(r_n = R) = 1$ (it must be $r_n \geqslant R$ for each chaser, otherwise the target is captured and the trial terminates). From equation (5), it is clear that the contribution to the escape term is larger for closer hounds, and that S can be interpreted as the effective 'viewing range' of the hare. The parameter v_e in equation (4) sets the maximum escape drift speed, which can be reached only asymptotically. By setting $v_e = 0$, the escape term $\boldsymbol{E}$ vanishes. We will refer to this situation as to that of a 'blind' target, the case which was previously studied in [51] and that we use for reference.

As in [51], we set $v_0 = 1$, which is equivalent to rescaling time units, and choose $R = 0.1$. The CT for each realization (trial) is a stochastic variable defined as

$$T_{d,N} = \min\left\{ t \,\middle|\, \min_{n=1,\ldots,N}\{\|\boldsymbol{X}(t) - \boldsymbol{Y_n}(t)\| \leqslant R\} \right\}. \tag{6}$$

The indices indicate the dimension of space, d, and the number of hounds, N. In the following, we will mainly focus on the mean CT, but will also briefly consider the median of the CT distribution.

Unless otherwise indicated, results of numerical simulations are based on the $M = 10^5$ realizations of equations (1) and (2) integrated with an Euler–Maruyama algorithm with time step $\Delta t = 10^{-6}$.

3. One-dimensional case

If hare and hounds move on a line, there can be at most two hounds, which start at $Y_{1(2)}(0) = \pm 1$. Furthermore, the hounds' trajectories do not depend on the particular noise realization, and are described by

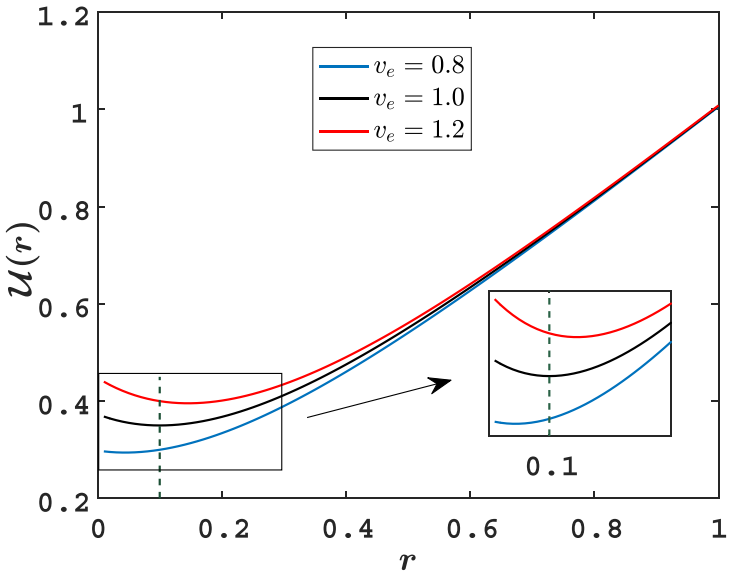

Figure 2. Examples of the potential function for the one-dimensional case, as in equation (10). Three values of the maximum escape velocity v_e are shown (blue, black, and red lines as indicated in the legend). The effective viewing range is here $S = 0.25$. Note that in this one-dimensional case the potential does not depend on the noise intensity D. The critical value $v_e = 1$ marks whether the capture occurs in a finite time in the noiseless system ($D = 0$).

$Y_{1(2)}(t) = \pm(1-t)$ (recall that the chasers' speed was set to $v_0 = 1$). When the number of chasers is $N = 1$, the simple variable transformation

$$r(t) = \|X(t) - Y_1(t)\|, \tag{7}$$

yields the Langevin equation for the distance between the single chaser and its target $r(t)$:

$$\frac{\mathrm{d}r}{\mathrm{d}t} = v_e g(r) - 1 + \sqrt{2D}\xi(t). \tag{8}$$

The stochastic dynamics of this distance can be regarded as the position of an overdamped Brownian particle

$$\frac{\mathrm{d}r}{\mathrm{d}t} = -\mathcal{U}'(r) + \sqrt{2D}\xi(t) \tag{9}$$

moving in the potential

$$\mathcal{U}(r) = r + v_e S \exp\left[-\frac{r-R}{S}\right] \tag{10}$$

with the initial condition $r(0) = 1$ and a fixed absorbing boundary at $r = R = 0.1$. We note that r is a positive quantity by definition. Furthermore, the absorbing boundary implies that r is always larger than R.

Examples of the potential function for different values of the escape speed are shown in figure 2; the magnified view in the inset reveals the position of the potential minimum with respect to the absorption point at $r = R$. Note that the potential is independent of the noise intensity, therefore, it makes sense to discuss the noiseless case $D = 0$ first. When $D = 0$, the motion of the hare follows deterministically the potential gradient, which only depends on $\boldsymbol{E}$ and is always directed away from the hound. The minimum of the potential function given in equation (10) is at

$$r_{\min} = R - S\ln\left(\frac{1}{v_e}\right). \tag{11}$$

The potential's minimum shifts to the right with the increase of v_e, as demonstrated by the three example curves in figure 2. When $v_e < 1$, the second term in equation (11), $\ln(1/v_e)$, is positive, resulting in a potential minimum at a value smaller than R (figure 2 blue line). This means that the boundary at $r = R$ is reached in a finite time even in the absence of noise—for sufficiently low escape speed (smaller than the pursuit speed of the hounds), capture is certain. When $v_e = 1$, the potential minimum is exactly at R (black

line). Here, technically, the CT in the deterministic case diverges already, since the passage to the smooth potential minimum takes an infinite time, as we show below (see equation (16)). For $v_e > 1$ an escape barrier is created by the potential that cannot be overcome in a noiseless system. Therefore, also in this case the CT diverges. Note that the critical condition for divergence ($v_e = 1$) is independent of the parameter S.

These qualitative considerations are confirmed by the solution of equation (8), which for $D = 0$ is an ordinary differential equation:

$$\frac{dr}{dt} = v_e \exp\left[-\frac{r-R}{S}\right] - 1 \tag{12}$$

with initial condition $r(t=0) = 1$. The change of variables $y = \exp(-r/S)$ can be used to transform the differential equation to

$$S\frac{dy}{dt} = y - v_e e^{R/S} y^2, \tag{13}$$

with initial condition $y(t=0) = e^{-1/S}$, which can be solved with standard methods. The solution is

$$y(t) = \frac{e^{t/S}}{e^{1/S} - v_e e^{R/S} + v_e e^{R/S} e^{t/S}}. \tag{14}$$

Thus, the explicit solution of equation (12) reads:

$$r(t) = -S \ln y(t) = S \ln\left[v_e e^{R/S} - \left(v_e e^{R/S} - e^{1/S}\right) e^{-t/S}\right]. \tag{15}$$

From equation (15), it is straightforward to obtain the deterministic CT

$$T_{\mathrm{Det}} = S \ln\left(\frac{e^{1/S} - v_e e^{R/S}}{1 - v_e}\right) - R, \tag{16}$$

which diverges for $v_e \to 1$ (we note that it must be $R < 1$ to avoid the trivial case of immediate capture).

A closed form for the mean CT can be found exactly also in the noisy case $D > 0$ because in equation (9) we are dealing with a one-dimensional homogeneous first-passage-time problem, for which the standard quadrature formula based on the backward Fokker–Planck equation can be applied [55]. Following this approach, the mean CT is given by

$$\langle T_{1,1} \rangle = \frac{1}{D} \int_R^1 dy \exp\left[\frac{\mathcal{U}(y)}{D}\right] \int_y^{+\infty} dz \exp\left[-\frac{\mathcal{U}(z)}{D}\right]. \tag{17}$$

Although the double integral in equation (17) cannot be performed analytically due to the nested exponential functions, the numerical evaluation of this expression can be compared to simulations as done in figures 3(a) and (b). Here, symbols indicate simulations and solid lines in the corresponding color represent the integration of equation (17). At very low noise intensities, the numerical integration of equation (17) becomes infeasible. Hence, the solid lines break off in the weak-noise limit, which will be dealt with by using different approximations, as discussed below.

In figure 3(a), the mean CT is shown as a function of the noise intensity D for $S = 0.25$ and several values of v_e as indicated in the legend. In the blind case $v_e = 0$, the mean CT is independent of the noise intensity and is just the mean first passage time of a Brownian motion with constant drift, given by $1 - R$ (black line, theory; black stars, simulations) [57]. When $v_e > 0$ the mean CT is always increased with respect to the blind case, as shown in figure 3(a) for the three values of v_e discussed above and in figure 2. It can be seen that all curves converge to the blind case in the strong-noise limit, whereas the behavior in the weak-noise limit depends on the value of v_e.

When the maximum escape speed is 'subcritical' (here represented by the case $v_e = 0.8$, purple diamonds), the mean CT converges to the deterministic limit given by equation (16), indicated by the purple horizontal dotted line. When the maximum escape speed is 'supercritical' (here we consider $v_e = 1.2$, blue circles), we know from the above discussion of the noiseless case that the potential has a minimum to the right of the absorbing barrier. Hence, the problem can be framed as an escape over a potential barrier, and we can find an approximation in the spirit of the classic Kramers escape formula [58]. If the noise is weak enough, we can expand the potential function in the first and second integrals in equation (17) as

$$\mathcal{U}(y) \approx \mathcal{U}(R) + \mathcal{U}'(R)(y - R), \tag{18}$$

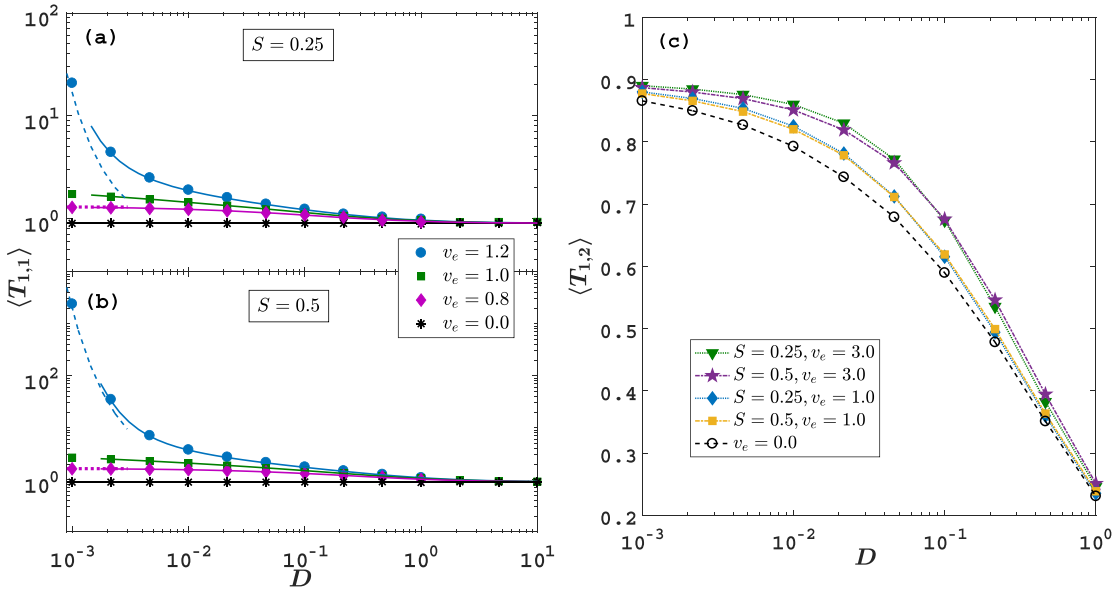

Figure 3. Mean capture time for the pursuit model in one dimension. (a) and (b): the mean capture time as a function of noise intensity D when $N = 1, S = 0.25$ (a) and $N = 1, S = 0.5$ (b). The values of v_e are indicated with various symbols and colors as in the legend. The analytical results (solid lines) are validated by numerical simulations (symbols). For very small noise intensities, the analytical results cannot be obtained because the numerical integration becomes unstable. The dotted lines represent the deterministic limit equation (16) when it is finite ($v_e = 0.8$). In the supercritical $v_e = 1.2$ the mean CT can be approximated by using the Kramers-like escape formula equation (20) (dashed line). (c): mean capture time as a function of D for $N = 2$ (symbols: running away under corresponding parameters; dashed lines: blindly diffusing cases).

$$\mathcal{U}(z) \approx \mathcal{U}(r_{\min}) + \frac{\mathcal{U}''(r_{\min})}{2}(z - r_{\min})^2, \tag{19}$$

respectively. We then employ a steepest-descent approximation [59, 60] to evaluate the inner integral (we extend the integration boundary to $\pm\infty$), and ultimately find the mean CT as follows

$$\begin{aligned}\langle T \rangle_{\mathrm{K}} &\approx \frac{1}{D}\int_R^1 \mathrm{d}y \mathrm{e}^{\frac{\mathcal{U}(R)+\mathcal{U}'(R)(y-R)}{D}} \int_{-\infty}^{+\infty} \mathrm{d}z \exp\left[-\frac{\mathcal{U}(r_{\min}) + \frac{\mathcal{U}''(r_{\min})}{2}(z - r_{\min})^2}{D}\right] \\ &= \frac{1}{D}\exp\left[\frac{\mathcal{U}(R) - \mathcal{U}(r_{\min})}{D}\right]\sqrt{\frac{2\pi D}{\mathcal{U}''(r_{\min})}}\int_R^1 \mathrm{d}y \exp\left[\frac{\mathcal{U}'(R)(y-R)}{D}\right] \\ &\approx \frac{\sqrt{2\pi D/\mathcal{U}''(r_{\min})}}{|\mathcal{U}'(R)|}\exp\left[\frac{\mathcal{U}(R) - \mathcal{U}(r_{\min})}{D}\right],\end{aligned} \tag{20}$$

where $\mathcal{U}(R) - \mathcal{U}(r_{\min})$ is the height of the barrier, i.e. the potential difference between the absorption point and the minimum. The result of this approximation, which is closely related to the transition time of an overdamped particle in a double-well potential [60], is shown in figure 3(a) as a blue dashed line.

The agreement with numerical simulations and the exact expression (blue solid line) becomes very good only when the noise intensity is sufficiently small compared to the potential barrier. The 'critical' case $v_e = 1$ cannot be handled by any of the two previous approximations. On the one hand, the potential's minimum is exactly at the barrier, and therefore no escape barrier is present regardless of how weak the noise intensity is. On the other hand, the deterministic CT diverges, hence it is not clear *a priori* whether the noisy case will diverge too. To deal with this case, we first decompose the mean CT as the sum of two terms. The first is the time necessary to reach a small distance ε from the capture boundary, which is a finite value that can be computed explicitly

$$T_{\mathrm{Det}}(1 \to R + \varepsilon) = S \ln\left(\frac{\mathrm{e}^{1/S} - v_e \mathrm{e}^{R/S}}{\mathrm{e}^{(R+\varepsilon)/S} - v_e \mathrm{e}^{R/S}}\right). \tag{21}$$

The second term is the time needed for the particle to reach the absorbing boundary at the potential minimum, when starting close to it, i.e. $\langle T(R + \varepsilon \to R) \rangle$. In this case, the potential can be approximated by a quadratic function. For this case, the mean first passage time is equivalent to the mean interspike interval of a leaky integrate-and-fire model [61, 62]

$$\langle T(R+\varepsilon \to R)\rangle = \sqrt{\pi}\int_0^{\frac{\varepsilon}{\sqrt{2D}}} \mathrm{d}x e^{x^2}\,\mathrm{erfc}\,(x), \tag{22}$$

where the upper integration boundary goes to infinity in the limit $D \to 0$. The integral in equation (22) diverges, as it can be shown by inserting the asymptotic expansion of the complementary error function for large argument $\mathrm{erfc}\,(x)\,e^{x^2} \sim 1/(x\sqrt{\pi})$, which leads to

$$\langle T(R+\varepsilon \to R)\rangle \sim K - \frac{1}{2}\ln(D), \tag{23}$$

where K is some constant of order one. Based on these approximations, it can be expected that the mean CT for $v_e = 1$ diverges very slowly as $D \to 0$.

When the effective viewing range is increased to $S = 0.5$ (figure 3(b)), the qualitative picture is unchanged. The mean CT is increased for all values of $v_e \neq 0$, and the range of validity of the weak-noise approximation equation (20) is wider because the potential barrier is larger.

When $N = 2$, an exact analytic solution is not easy to find, since the variable change equation (7) leads to a time-dependent potential, which prevents using the analytic approach discussed until now for the case $N = 1$. Also the method of images used in [51] is not viable here, since the solution to the free diffusion equation clearly does not solve equation (1) in general, but only when $v_e = 0$.

The mean CT from numerical simulations is shown in figure 3(c). Since the hare is trapped between the two hounds, the (mean) CT cannot be larger than the time at which the two chasers hit the fixed interval $(-R, R)$ (the one-dimensional circle), which is at time $1 - R$. This time is also the deterministic limit for all values of v_e, because for symmetry the escape term is always zero. Increasing the noise term can only reduce the CT, since it can only push the hare toward either chaser. Hence, the mean CT decreases upon increasing D for all values of v_e. The escape term is always pointing to the origin, and its effect is mostly noticeable at intermediate noise levels, at which the displacement from the origin caused by the noise term can be countered by the escape term, which acts as a restoring 'force'. At strong noise, all drift terms become irrelevant and all curves converge to the blind case, which goes to zero as $D \to \infty$ [51]. The simulation results of figure 3(c) also show that when v_e is fixed, the parameter S has little effect on the mean CT, whereas the increase of v_e has a much more evident effect on the mean CT compared to the blind case.

4. Two-dimensional case

When hounds and hare can move in a two-dimensional space, the initial conditions become $\boldsymbol{X}(0) = (0, 0)$, and $\boldsymbol{Y}_n(0) = (\cos\frac{2\pi n}{N}, \sin\frac{2\pi n}{N})$. In words, the chasers are placed at evenly spaced angles on a ring of radius one. Although in principle the number of chasers can be arbitrarily large, if the chasers are so many that their initial positions are less than $2R$ apart from each other, an inescapable ring is formed, which leads to almost identical CT distributions when N is larger than a certain value[6]. When $R = 0.1$, this maximum number of chasers is $N_{\max} = 32$. In the following, we will discuss the case $N = 1$ first, which can be solved analogously to the one-dimensional case.

4.1. One chaser

When there is only one hound ($N = 1$), the system is best described in polar coordinates centered on the hound's position:

$$\boldsymbol{X}(t) - \boldsymbol{Y}_1(t) = \begin{pmatrix} r(t)\cos\phi(t) \\ r(t)\sin\phi(t) \end{pmatrix}, \tag{24}$$

where

$$r(t) = \|\boldsymbol{X}(t) - \boldsymbol{Y}_1(t)\|. \tag{25}$$

By applying Itô's lemma for the change of variables, equations (1) and (2) can be transformed to a pair of Langevin equations with independent variables $r(t)$ and $\phi(t)$. Since the capture condition $r(t) = R$ does not depend on ϕ, only the r equation matters, which is

[6] The distance between any two given chasers can never grow in the present model, but can at most stay constant (this happens when the target is aligned with the line connecting the two considered chasers, but it is not between them). Since all distances between closest chaser pairs are already smaller than the gap needed to escape at the beginning, no exit from the ring is possible. Hence, all trajectories will be trapped inside a highly symmetrical 'tightening noose' [51]. Still, adding more chasers beyond the 'maximum' N can still marginally decrease the CT, because the space occupied by the absorbing boundary becomes slightly larger (the ring of hounds becomes slightly 'thicker').

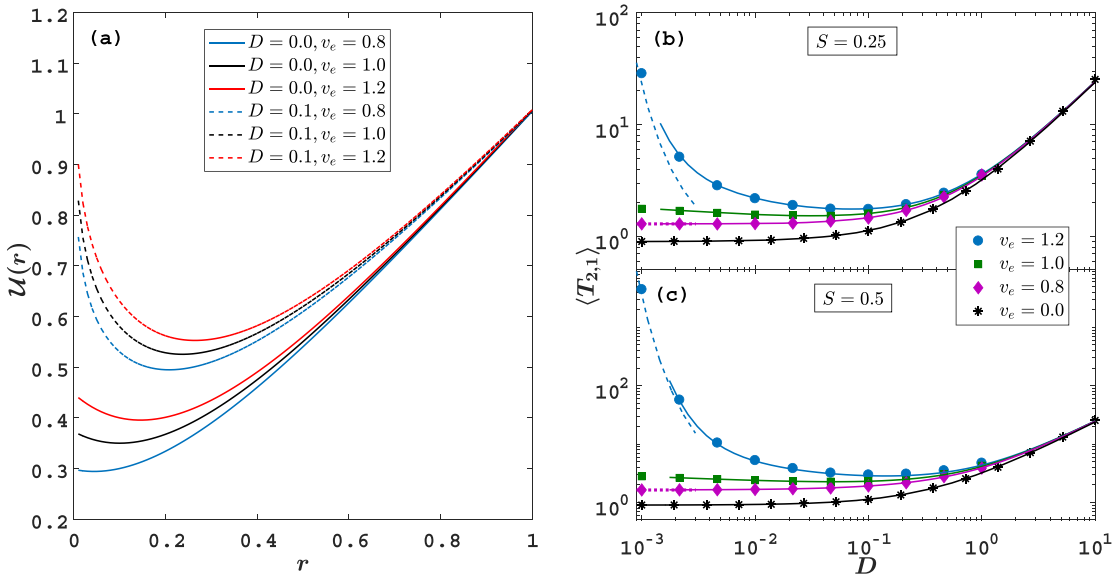

Figure 4. Pursuit model in two dimensions and a single chaser. (a) The potential function for three values of v_e (blue, black, and red lines as indicated in the legend) and for intermediate noise strength $D = 0.1$ (dashed lines) and $D = 0.0$ (solid lines). The effective viewing range is here $S = 0.25$. (b) and (c): The mean CT as a function of noise intensity D for $d = 2, N = 1$ for $S = 0.25$ (b) and $S = 0.5$ (c). The analytical results (solid lines) are validated by numerical simulations (symbols). At small noise intensities, the analytical results cannot be obtained due to instability of the numerical integration. The deterministic limit for subcritical value $v_e = 0.8$ (dotted lines) and the Kramers-like approximation equation (20) for supercritical $v_e = 1.2$ (dashed line) are used in the weak-noise limit (see also figure 3 and corresponding discussion in the main text).

$$\frac{\mathrm{d}r}{\mathrm{d}t} = \sqrt{2D}\xi_r(t) + v_e g(r) - 1 + \frac{D}{r}. \tag{26}$$

Hence, the problem admits an effectively one-dimensional description, i.e. that of a particle that starts at $r(0) = 1$ and diffuses in the potential

$$\mathcal{U}(r) = r - D\ln(r) + v_e S \exp\left[-\frac{r-R}{S}\right], \tag{27}$$

until the exit boundary at $r = R = 0.1$ is reached.

Again, we start considering the noiseless case. Note that if $D = 0$, the potential function becomes the same as for the one-dimensional case, equation (10). Thus, the critical condition for divergence in the deterministic two-dimensional case is still $v_e = 1$, the deterministic CT is still given by equation (16), and the discussion of the one-dimensional capture process still applies. This is not surprising because without noise in the two spatial directions, the capture process takes place along the first connecting line between the hare and the single hound, i.e. practically in one spatial dimension.

When $D > 0$, the additional noise-induced (or Stratonovich) drift term $-D\ln(r)$ increases the potential in equation (27) at small r, and thus shifts the minimum to the right, compared to the noiseless case[7]. This effect is visualized in figure 4(a): see the dashed lines compared to the solid ones of the same color.

The additional noise term does not alter the problem fundamentally with respect to the one-dimensional case discussed above. In particular, the exact expression for the mean CT equation (17) still applies. In the specific case $v_e = 0$, the integral can be computed exactly and gives the elementary solution given in [51]

$$\langle T_{2,1}(D) \rangle|_{v_e=0} = 1 - R + D\ln\left(\frac{1}{R}\right). \tag{28}$$

Otherwise, equation (17) needs again to be integrated numerically, which is feasible for all values of D that are not too small.

[7] The reader might be puzzled that we mention and discuss a Stratonovich drift term that is usually associated with a *multiplicative* noise (a noise with state-dependent amplitude), although our original system contains only *additive* (state-independent) noise. The explanation lays in the nonlinear transformation to polar coordinates that turns the additive noise into a multiplicative one that, in the so-called Stratonovich interpretation of the stochastic differential equation, comes along with a deterministic drift term, the above mentioned Stratonovich drift [55]. For a similar case and a more thorough discussion of the issue, see [56].

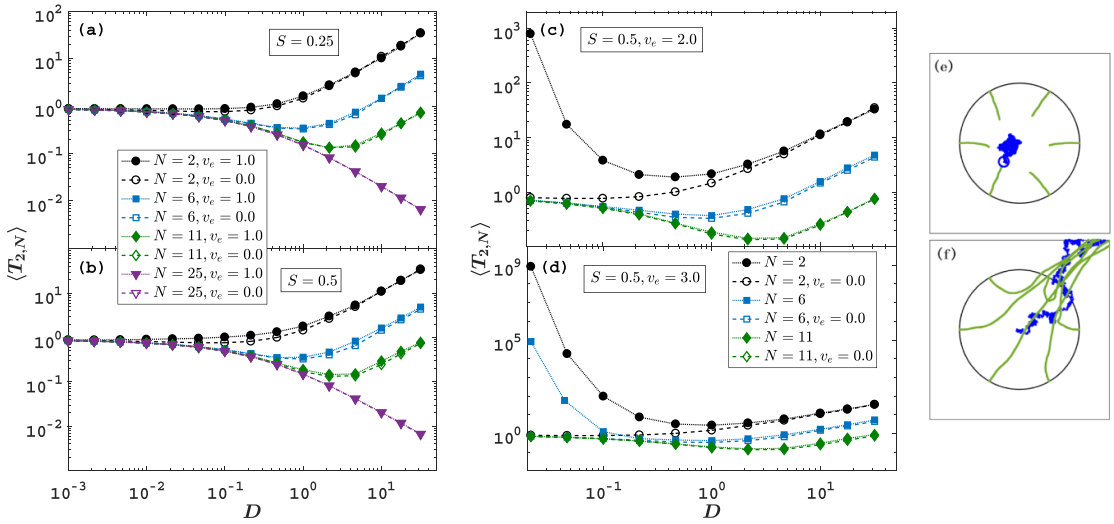

Figure 5. Results of pursuit model in two dimensions with multiple chasers: for each value of N, there is a v_e above which the repulsion term causes the mean CT at weak noise to increase dramatically (black lines in (c), black and blue lines in (d)). Below this critical escape speed, there is barely any difference to the blind case. The mean capture time is shown as a function of noise intensity D for $N \geqslant 2$ (closed symbols: actively running prey with speed $v_e = 1$; open symbols and dashed lines: corresponding blind prey) and $S = 0.25$ (a) and $S = 0.5$ (b). The escape speed is set to the two supracritical values $v_e = 2$ and $v_e = 3$ in (c) and (d), respectively. Note that when $v_e \neq 0$, a numerical/analytical 'hybrid' method was used to deal with trajectories that run for an exceedingly long time, as described in the main text (last paragraph of section 4.2). Two realizations for $N = 6, D = 0.1, v_e = 3.0$ are shown in (e) and (f). Here, the green curves are the hounds' trajectories, and the blue curves are the hare's trajectories, respectively. The prey can be captured either inside or outside the initial circle, which correspond to the cases of an ensnared trajectory (e), and of an 'escapee' (f), respectively.

The comparison between the analytical expression for the mean CT and Monte Carlo simulations is shown in figures 4(b) and (c). At low noise, all curves are almost identical to the one-dimensional case, as it is expected since in the weak-noise limit the potential function approaches the one in the one-dimensional case. At stronger noise, all curves bend upwards and converge to the same line, which coincides with the blind case $v_e = 0$, which can be also expected because in the limit $D \to \infty$ both deterministic drift terms are less and less relevant (they can be made arbitrarily small through a rescaling of the time units).

The mean CT is apparently increased for relatively weak noises when comparing to the case of a completely random prey, indicating that the survival time of the hare is efficiently increased when it can run away from the hound and the noise intensity is small. Intuitively, the hare can survive longer with larger S, for a given v_e.

4.2. Multiple chasers

When $N \geqslant 2$, the hounds start on the unit circle centered on the hare's position (the origin) and are equidistant from each other. In this section, we show the mean CT as a function of the noise intensity D for several sets of parameters to discuss the effects of S and v_e on prolonging the survival time of the hare. The results in this section are obtained by means of numerical simulations.

When the maximum drift speed of the hare v_e is as large as the hounds' speed ($v_0 = 1$), the repulsion force has little effect on the mean CT. In figures 5(a) and (b), dotted lines with closed symbols represent the mean CT for the situation in which the hare can 'actively run' (i.e. $v_e \neq 0$), while results for the corresponding 'blindly diffusing' cases are shown as dashed lines and open symbols. Two distinct values of S are considered in the first two panels of figure 5. Specifically, figure 5(a) contrasts the blind case to the case of $v_e = 1$, i.e. when the maximum escape drift is equal to the chasers' speed and $S = 0.25$. Remarkably, the escape term has hardly any effect regardless of the number of chasers, which range from $N = 2$ to $N = 25$. If the viewing range is increased to $S = 0.5$ (figure 5(b)), some increase in the mean CT can be seen in the intermediate-noise and strong-noise range, but the difference is rather limited.

Looking back at figure 4 in last subsection, when $N = 1$ and $v_e = 1$ the mean CT can be twofold (when $S = 0.25$) or threefold (for $S = 0.5$) of the blind case in the weak and middle noise range. However, the results of figures 5(a) and (b) show that when $N \geqslant 2$ running away barely affects the hare's mean survival time. The reason for this surprising finding is the symmetry in the initial conditions: The contributions of each chaser to the total 'repulsion term' tend to cancel each other, so that the repulsion term $\boldsymbol{E}$ is close to 0. For weak and moderate noise the amount of 'symmetry breaking' (the hare's typical displacement from the origin) is also small, so that the total $\boldsymbol{E}$ stays small during the entire trial when it is captured, which is the same as that for

blindly diffusing cases. And when the noise is strong, the system is dominated by the noise, so that running away from the chasers does not affect the mean CT compared to the blindly diffusing cases.

We now consider the case that v_e is larger than 1, in which the $N = 1$ case shows a divergence of the mean CT when $D \to \infty$. Figure 5(c) shows simulation results for the mean CT as a function of D for $S = 0.5$ and $v_e = 2$ (solid lines and closed symbols); the values of N are indicated in the legend. Again, the reference case $v_e = 0$ is represented with dotted lines and open symbols. Here, a striking difference is observed between the two scenarios when $N = 2$ (figure 5(c) black circles and lines); at weak noise, the mean CT diverges for $D \to 0$ when the hare is actively running away from its pursuers ($v_e = 2$), as opposed of the blind case ($v_e = 0$) for which $\langle T_{2,N} \rangle$ saturates at the finite value $1 - R$. If, however, the number of hounds is increased to $N = 6$ (blue squares) or $N = 11$ (green diamonds) the difference to the blind case is, once more, very small. When the maximum escape speed is further increased to $v_e = 3$ (figure 5(d)), the same qualitative behavior observed in figure 5(c) for $N = 2$ (divergence for $D \to 0$, increase of the first derivative at $D \to \infty$) is observed here also for the case of $N = 6$ (blue squares and solid lines), whereas simulation results for $v_e = 0$ and $v_e = 3$ are still very similar when $N = 11$.

The system's behavior at weak noise can be interpreted as follows: in the initial position, the evasion term $\boldsymbol{E}$ is zero, since all contributions cancel out for symmetry. As the chasers get into the effective viewing range, some displacement from the origin due to the noise term will have broken the symmetry. If this random displacement occurs towards one of the chasers, the evasion term will push back the hare towards the origin, where it is eventually captured (an example of these 'ensnared' trajectories is shown in figure 5(e)). This kind of trajectories will have a mean CT that is only marginally larger than in the blind case, since the symmetry is roughly conserved during the entire realization, and hence the escape term is mostly negligible during the entire trajectory. If, however, the random displacement from the origin due to noise occurs into an 'escape corridor', i.e. the region between two neighboring chasers, the trajectory can escape the initial ring, as in figure 5(f). In this case, the chasers form a pack and effectively act as a single one. In this kind of 'escaped trajectories', the mean CT is much longer and diverges in the limit $D \to 0$. These escaped trajectories account for the growth of the mean CT at low noise. Clearly, the size of this 'escape corridor' and, hence, the probability of an escaped trajectory depend both on the number of chasers: more chasers reduce the probability of escaping, whereas a larger v_e increases it, which explains the differences between the two cases observed in figures 5(c) and (d) at weak noise.

We conclude this section on a technical note. As discussed above, at weak noise and $v_e > 1$, the behavior of the mean CT is determined by whether rare realizations can escape the ring of hounds. These trajectories can run for an extremely long time, which poses also a technical challenge in terms of numerical simulations. To deal with this problem, we used a 'hybrid' method to calculate the mean CT for $v_e = 2$ and $v_e = 3$ in figures 5(c) and (d), and in the following figures 8(c) and 9(d): We fixed a threshold time $T_{\max} = 10^6$. If this time is reached in a given trial and the hare is still not captured, it is a clear indication that this realization has 'escaped'. In this case, the analytical value for the mean CT for $N = 1$ and the corresponding parameters as given in equation (17) is used as CT for this particular trajectory, assuming that the time it took for the hare to exit the circle and reach the 'point of equilibrium' during pursuit is negligible compared to the very long CT. A further assumption is that the mean CT for escaped trajectories is representative of the single trajectory (at least with respect to the order of magnitude). In the next subsection, we investigate in more detail how these rare trajectories can cause a qualitative shift in the mean CT.

4.3. Critical escape velocity

The results shown in figure 5 suggest that the system's behavior in the weak noise range undergoes an abrupt transition when v_e is increased beyond some value. We argued that this transition is due to few rare trajectories, which escape the initial circle and for which the CT is very large. In other words, the statistical ensemble can be split into two parts and the mean CT can be written as

$$\langle T_{2,N} \rangle = p_{\mathrm{esc}} \langle T_{2,N} \rangle_{\mathrm{esc}} + (1 - p_{\mathrm{esc}}) \langle T_{2,N} \rangle_{\mathrm{not\,esc}} \approx p_{\mathrm{esc}} \langle T_{2,1} \rangle_{\mathrm{esc}} + 1, \tag{29}$$

where p_{esc} is the probability of observing escaped trajectories, $\langle T_{2,N} \rangle_{\mathrm{esc}}$ is the mean CT of these trajectories, and $\langle T_{2,N} \rangle_{\mathrm{not\,esc}}$ is the mean CT of trajectories that do not escape the initial circle. In the approximation, we have used that (a) for weak noise $p_{\mathrm{esc}} \ll 1$; (b) the mean CT of escaped trajectories depends only marginally on the number of chasers; (c) the mean CT of trajectories that do not make it out of the initial circle is of order unity. Hence, at weak noise the mean CT is determined by the behavior of $\langle T_{2,1} \rangle_{\mathrm{esc}}$ and p_{esc} as a function of the system's parameters, and, in particular, of v_e, D, and N.

As a first remark, in the noiseless case ($D = 0$) the circular symmetry of the problem causes the hare to be motionless, which leads to capture after $1 - R$ time units. Hence, a nonvanishing noise intensity is required

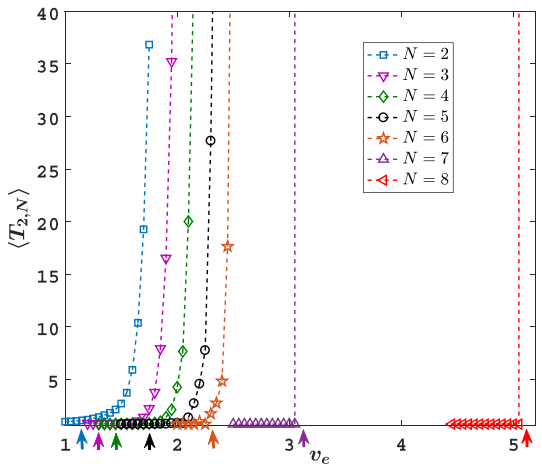

Figure 6. In the weak-noise regime, the mean CT undergoes a strong increase if v_e is increased beyond a 'critical' value. The plot shows the mean CT for weak noise ($D = 0.02$) as a function of v_e for several values of N, as reported in the legend. For each curve an arrow in the same color marks the critical value $v_{e,crit}$, which is defined as the smallest v_e for which at least one trajectory escapes the initial circle and reaches a distance 10 from the origin. This escape criterion is used here for the 'hybrid' method to calculate the mean CT (see section 4.2). The total number of trajectories used here is the standard value $M = 10^5$. Note that $v_{e,crit}$ depends, in general, on D, on the discretization of v_e (here 0.05), and on the size of the ensemble M (see figure 7(j) and (related) discussion).

to observe an *escape-from-the-circle* event. To investigate this phenomenon more systematically, we choose the weak noise intensity $D = 0.02$, and we measure the mean CT from $M = 10^5$ of trials as a function of v_e for several values of N. Indeed, figure 6 shows that the mean CT increases sharply at a value that depends on N. This behavior suggests that the 'critical' escape speed $v_{e,crit}$ should be taken close to the value of v_e at which the curve of the mean CT 'takes off'. Based on our assumption that the sharp increase is due to trajectories that escape the hounds' circle, a more precise definition of $v_{e,crit}$ is to take the smallest v_e for which at least one 'escaped' trajectory (out of M) is observed, which will be the criterion used in the following. A trajectory will be considered to have escaped the initial ring if a distance ten (measured in multiple of the starting distance between chasers and target) from the origin is reached. In figure 6, for each curve the value of $v_{e,crit}$ is marked by a vertical arrow in the same color of the corresponding N. For larger values of N, the increase is extremely sharp, and $v_{e,crit}$ is at the jump's location. For smaller values of N, the mean CT undergoes a smoother transition. In this case, $v_{e,crit}$ is somewhat smaller than the point of maximum growth, but it marks the position where the curves start to bend up.

The results in figure 6 suggest that $v_{e,crit}$—defined as the smallest v_e for which at least an escape is observed—marks reasonably well the point of qualitative change in the system's behavior, and that $v_{e,crit}$ grows on increasing N. As a way to further substantiate the intuition about how N and v_e influence the probability of observing an escaped trajectory, the idea of the 'escape corridors' introduced in the previous section is visualized in figure 7. More specifically, figures 7(a)–(i) show the starting positions for the hare that, in the deterministic system ($D = 0$), lead to capture (red areas) and escape (blue areas), respectively.

Consider, for concreteness, the case $N = 3$ and $v_e = 2$, depicted in figure 7(a). For non-zero but weak noise, most random displacements due to the driving noise will push the hare mostly to a position which is still in the vicinity of the origin. These positions are all 'red' (i.e. they ultimately lead to capture in the deterministic system) for all N; hence, from these positions the deterministic drift will most likely bring the hare back toward the origin. In this case, the symmetry of the problem will be maintained, and the hounds will close in such that, at a later time point, the system's configuration will likely be close to figure 7(b), and afterwards to that depicted in figure 7(c). It can be seen that the red region keeps shrinking until the black areas (that represent the capture area) touch each other and escape is then impossible. Until this time, however, a rare noise fluctuation can drive the hare into the blue region, from which the deterministic drift is likely to push the hare away, thus leading to an escaped trajectory. We note that the escape is most likely through the saddle points of the effective potential created by the hounds' presence. Indeed, these points of minimal distance of the blue region to the origin are the 'holes in the net' through which the hare is most likely to slip through, and the potential difference between the saddle point and the origin could be loosely defined as an effective escape barrier, the height of which, due to the hounds' motion, depends on time. If v_e is increased, this qualitative description of the system's evolution will still apply, but the blue region expands closer to the origin, thus increasing the probability of an escape (figures 7(d)–(f)). Intuitively, increasing the

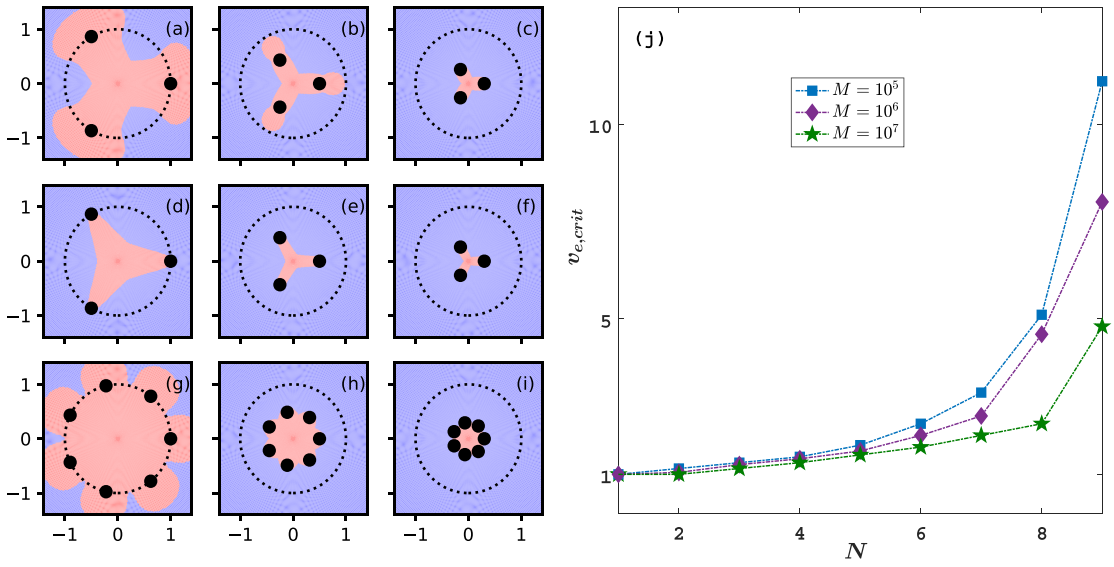

Figure 7. The effective escape barrier is lowered by increasing $v_{e,crit}$, and it grows by increasing N. Furthermore, the value of $v_{e,crit}$ depends on the size of the ensemble. Panels (a)–(i) represent the deterministic system's evolution, in which the red and blue area mark the initial positions from which the hare is ultimately captured or escapes, respectively. Parameters: (a)–(c) $N = 3$, $v_e = 2$; (d)–(f) $N = 3$, $v_e = 3$; (g)–(i) $N = 7$, $v_e = 3$. Panel (j): critical velocity $v_{e,crit}$ vs. number of chasers N for different numbers of trials M as indicated. Other parameters: $D = 0.02$.

number of chasers has the opposite effect, i.e. it makes the 'red' area grow, and it could be seen as enhancing the height of the effective escape barrier (figure 7(g)–(i)). It is worth remembering that, when N is so large that the black capture region becomes connected (this happens for $N = 32$ with our standard choice $R = 0.1$), escape is not possible, and $v_{e,crit}$ cannot be defined in a meaningful way.

The above discussion makes clear that $v_{e,crit}$ is the value of v_e for which the effective escape barrier is so low that the probability of escaping through the saddle point p_{esc} becomes of order $\sim 1/M$, where M indicates the number of trials. Consequently, $v_{e,crit}$ will depend on the size of the statistical ensemble. Until now, the behavior of $v_{e,crit}$ has been investigated for the standard ensemble size used in all other figures ($M = 10^5$). The effect of increasing the number of realizations is visualized in figure 7(j). Indeed, the critical v_e displays a decreasing trend with M for all N. Figure 7(j) shows that, for a fixed M, $v_{e,crit}$ increases very steeply with N. These points are, however, also those that are most sensitive to the ensemble size.

The results in figure 7(j) indicate that $v_{e,crit}$ decreases toward unity for all N, which begs the question whether, in the limit $D \to 0$ and $M \to \infty$, the critical value will tend to one for all N. According to the definition of $v_{e,crit}$ as the lowest v_e for which an escape from the circle is observed, in the limit $M \to \infty$ there is a nonzero probability of reaching *any* distance from the origin because the driving noise is unbounded. Of course, the number of realizations needed to observe at least one such event grows without bound as well, when $D \to 0$. Hence, $v_{e,crit}$ will eventually decrease to $-\infty$ if $M \to \infty$. In this case, however, $\langle T_{2,N} \rangle_{esc}$ is finite, so that the mean CT, according to equation (29), will not grow. Indeed, it makes sense to limit $v_{e,crit}$ to the interval $[1, \infty)$. Even in this case, however, the behavior of the indeterminate form 'zero times infinity' in equation (29) is hard to predict when $M \to \infty$ and D is arbitrary small. The factor $\langle T_{2,N} \rangle_{esc}$ can be expected to diverge as $\sim \exp(\Delta \mathcal{U}_e / D)$, where $\Delta \mathcal{U}_e$ is the effective barrier height during the pursuit (after the escape). The limiting behavior of the escape probability p_{esc}, however, is harder to predict. Framing this problem as an escape over an effective barrier suggests that the asymptotic behavior will be $p_{esc} \sim \exp(-\Delta \mathcal{U}_b / D)$. In the end, the limiting behavior of the product $\langle T_{2,N} \rangle_{esc} \cdot p_{esc}$ may depend both on the precise value of the effective escape barrier and on the prefactors, which is a challenging problem to tackle analytically. This discussion makes also clear that a very slow convergence to the limiting value is to be expected, so that even a numerical investigation of the problem is hard.

In summary, there is some degree of unsolved ambiguity in the above definition of the critical v_e, or rather in the behavior of the mean CT in the limit $M \to \infty$ and arbitrarily small D. We emphasize that, however, for any sufficiently large ensemble size and sufficiently small but finite noise level, the definition of $v_{e,crit}$ yields results that are reasonable and consistent. The fact that an extremely rare event can possibly cause an abrupt change in the mean CT is a curious mathematical problem but it would make no practical difference in most physical situations. Indeed, this mathematical inconsistency begs the question of whether the mean CT is the most meaningful statistical property to be considered in this weak-noise regime. This issue is discussed further below, in section 4.5.

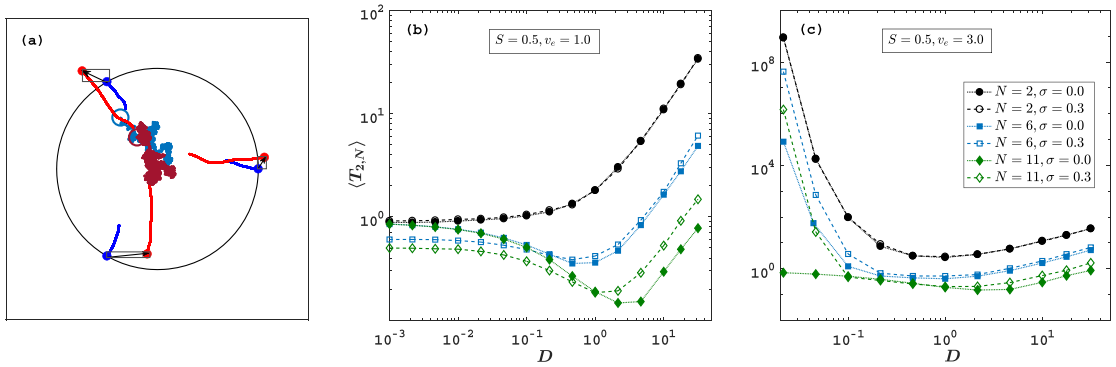

Figure 8. Effect of randomized starting positions of the pursuers: for $v_e = 1$ (b), the random starting positions increase the mean CT at strong noise and decrease the mean CT at weak noise; for larger v_e (c), the mean CT increases strongly at weak noise by a randomization of the initial positions. Two realizations for $N = 3, D = 0.1, v_e = 1.0$ are shown in (a). The blue trajectories represent the hounds start with equidistant arrangement over the unit circle ($\sigma = 0$). Red trajectories show the case of randomized starting positions (here $\sigma = 0.2$). The mean CT as a function of noise intensity D with deterministic (solid lines) and random initial positions of the hounds (dashed lines) are compared in (b) and (c) in the cases of $v_e = 1$ and $v_e = 3$. The results in (c) include trajectories handled with the 'hybrid' simulation method (see last paragraph of section 4.2).

4.4. Random starting positions

Since the circular symmetry of the chasers' initial positions plays an important role in the finding that even a strong escape term has hardly any effect when multiple chasers are present, it is natural to ask how disrupting this symmetry can change the picture. To this end, we will add a random component to the initial positions of each hound and explore how the mean CT is affected in the remainder of this section. These random components will be i.i.d. Gaussian numbers with zero mean and standard deviation σ. Hence, the starting position of the nth hound is now

$$\boldsymbol{Y}_n(0) = \left(\cos\frac{2\pi n}{N} + u_1, \sin\frac{2\pi n}{N} + u_2 \right) \tag{30}$$

where are $u_1, u_2 \sim N(0, \sigma^2)$. Note that σ is here the standard deviation of the single component and not of the random vector $\boldsymbol{Y}_n(0)$, and that when $\sigma = 0.0$ the non-random initial conditions used so far are recovered. Figure 8(a) shows an example trajectory of a trial with randomized initial components (red) compared to the fixed initial conditions (blue).

We will focus on the case $S = 0.5$ and $v_e = 1$ first, for which the escape term has hardly any effect on the mean CT compared to the blind case. Figure 8(b) contrasts the simulation results obtained with randomized initial conditions (open symbols and dashed lines) and the case of fixed initial conditions $\sigma = 0$ (open symbols and dotted lines). When $N = 2$ the curves corresponding to the two cases (black open/close circles and dashed/dotted lines) are almost indistinguishable, indicating that the random shifts of the hounds' initial positions has little effect on the mean CT. When the number of chasers is increased to $N = 6$ (blue squares and lines), an effect can be seen: the mean CT is decreased for weak noises when the starting positions of the hounds are random ($\sigma = 0.3$), and it is slightly increased at larger noise intensities with respect to the nonrandom initial conditions ($\sigma = 0$, open squares and dotted lines). The same qualitative difference is observed in a more pronounced fashion if the number of chasers is increased to $N = 11$ (green diamonds). These observations can be interpreted as follows. In the weak-noise limit, the CT is approximately equal to distance to the closest chaser. If there are enough chasers, the probability of reducing the initial distance of one of the chasers outweighs the probability of increasing it. In the strong-noise limit, the deterministic escape speed plays a minor role, and the increase in the mean CT is dominated by the trajectories that slip through the ring of hounds [51]. In this scenario, the random initial conditions can lead to a wider hole in the 'net of chasers', and thus increase the probability that a trajectory can slip through.

We can now consider the case of 'supracritical' escape velocity $v_e = 3$ (figure 8(c)). Also in this case no appreciable difference can be seen between random and fixed initial conditions when $N = 2$ (black circles and lines), and the mean CT has the same behavior observed in the previous section. When the number of chasers is increased to $N = 6$, however, the random initial conditions lead to a difference, namely, an increase in the mean CT at all noise levels (open vs. closed blue squares). When $N = 11$ (green diamonds), the randomized initial conditions cause the mean CT to diverge in the vanishing noise limit (open diamonds) whereas the fixed initial conditions lead to a finite mean CT (closed green diamonds); otherwise, the random initial conditions cause a modest increase in the mean CT.

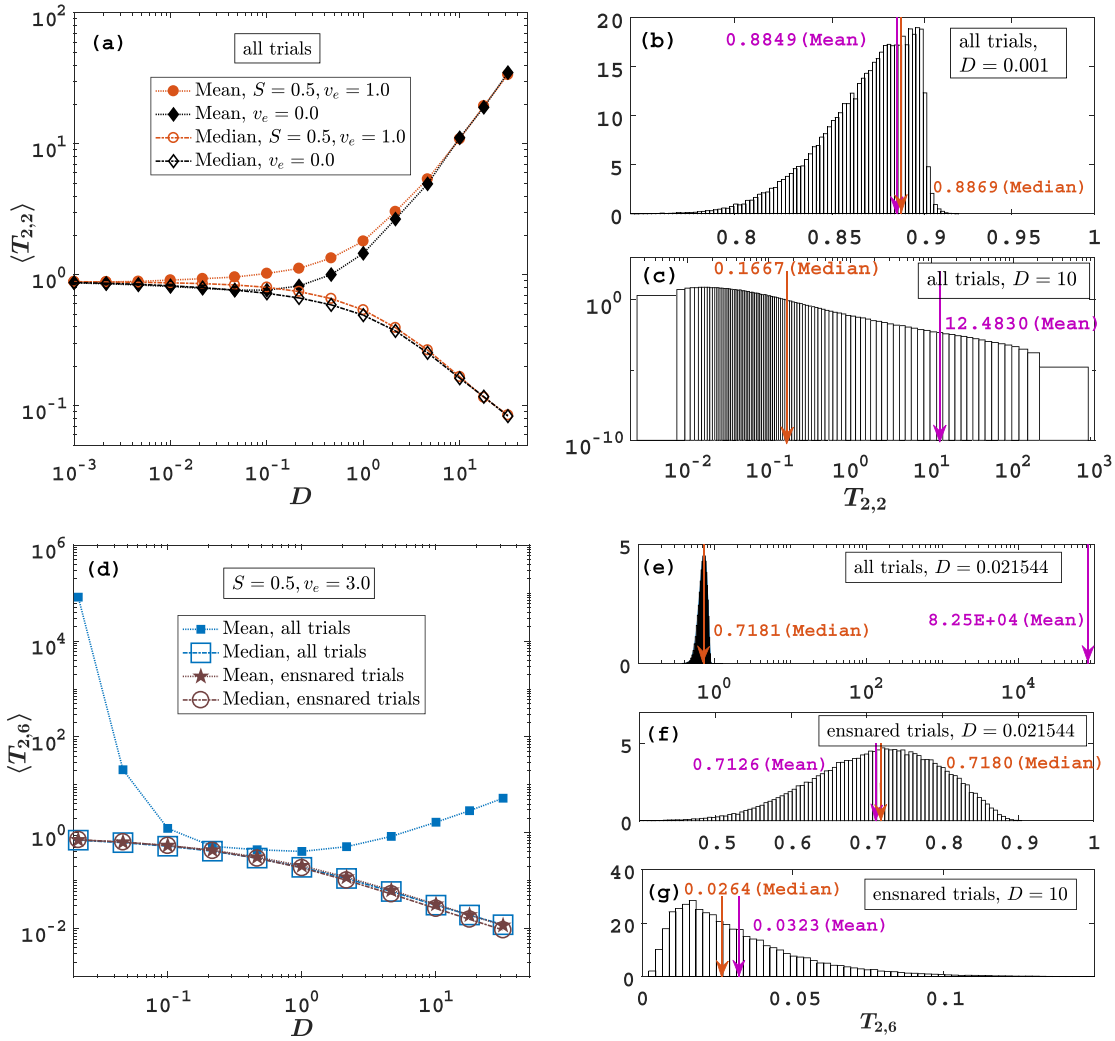

Figure 9. At very weak or very large noise intensity, the mean capture time is dominated by rare events. The mean and median used to estimate the mean capture time as a function of noise intensity D for $N = 2$ and $N = 6$ are compared in (a) and (d), respectively. The distributions of the capture time are shown in the remaining panels to illustrate the reason for the differences between average and median. Parameters: $N = 2, v_e = 0$ (b) and (c), $N = 6, v_e = 3$ (e)–(g). Only the trajectories that are captured before leaving a circle of radius 10 around the prey's initial position (ensnared trials) are considered in (f) and (g), in this case the mean and median coincide again.

In summary, the random initial conditions have a different effect on the mean CT for weak noise depending whether v_e is above or below the critical value: If it is below or near the critical value and there are sufficiently many chasers, as in figure 8(b), it can lead to a reduced mean CT because there is a sizable chance that one of the chasers starts closer to the hare; If it is above the critical value, it can only increase the mean CT because it enhances the chances that a wider 'escape corridor' is formed between a couple of chasers. For the same reason, the mean CT is always increased by the random initial condition, although here the escape through the hound pack is driven by noise [51].

4.5. Mean and median

So far, the mean CT was considered as the only statistics of interest. However, in several circumstances the mean CT is dominated by rare outliers with extremely large CT, while most trajectories have a CT that is orders of magnitude smaller. In this case, the mean is perhaps not the most appropriate way to characterize the statistical ensemble. In this last subsection, we will investigate the median as an alternative way of characterizing the typical CT. The median is given by the time that splits the full CT probability density into equal halves (or, equivalently, the time at which the cumulative probability distribution reaches 0.5). For brevity, we will focus on a selection of emblematic cases.

In figure 9(a), the mean and median CT as a function of D are compared for $N = 2$, $S = 0.5$, and v_e is either equal to zero or $v_e = 1$. Here, all curves are rather similar to each other in the weak-noise range. However, as the noise level grows, the mean CT increases (black circles) whereas the median CT decreases

(orange squares). This applies to both the blind (empty symbols) and the sighted prey (closed symbols). Looking at the histogram of the CT at weak noise (figure 9(b)) makes clear the reason why mean and median are close to each other: although the CT distribution has a peculiar skewed shape with a sharp drop around the deterministic CT (here, $v_e = 0$), it is clearly unimodal with no heavy tails. In contrast, when the noise is strong, the CT distribution is spread over several orders of magnitude with a heavy tail (figure 9(c)), which shifts the mean to the right, although half of the distribution is concentrated at rather low values and the majority of realizations has typically much smaller values than the mean value.

In the 'supracritical' maximum speed range (figure 9(d)), the mean (closed squares) and the median CT are only similar in the intermediate noise range. At strong noise, the situation is similar to that discussed in the previous paragraph. At weak noise, however, mean and median CT are also very different from each other. The mean increases without bound for $D \to 0$, as already seen in the previous subsection, whereas the median saturates at a finite value. The CT histogram (figure 9(e)) demonstrates that all but few rare CT are concentrated around the median CT. However, the CT of the rare 'escapees' is so much larger that the mean is about five orders of magnitude larger than the median. If the escaped trajectories are left out and only ensnared trajectories are considered, mean and median are rather close to each other at all noise intensities (figure 9(d), compare filled stars with open circles, and the CT distributions in figures 9(f) and (g)). In the weak-noise regime, the median seems to better represent the CT of the typical trajectory, although it misses the information about the rare events. In the strong-noise regime, the difference is more nuanced, since the distribution is more skewed and the weight of the right tail is larger.

5. Concluding remarks

In the present study, we have investigated how a recently proposed stochastic pursuit model is changed by the addition of a deterministic 'repulsion term' that drives the prey away from the chasers.

For the case of one chaser, we could derive an analytical expression for the mean CT in the form of a double integral which can be easily evaluated numerically for most parameter values and further simplified in special limit cases. These analytical results were validated by numerical simulations. The case of several chasers was studied by simulations only.

The 'repulsion' or 'escape' term introduced here has two parameters: the effective viewing range S and the maximum escape speed of the hare v_e. In all considered scenarios, the viewing range S had a minor effect on the mean CT. On the contrary, the maximum escape speed v_e could trigger a qualitative change in the mean CT's behavior as a function of the noise intensity D. In particular, it was found that when v_e is not large compared to the hounds' speed (here set equal to one), running away based on the given repulsion force caused only minor consequences for the hare's survival time: a moderate increase at weak noise if there is only one chaser ($N = 1$), or hardly any effect when $N \geqslant 2$. This rather surprising result holds true also when $v_e = 1$ (i.e. the maximum escape drift speed is equal to the chasers' speed), and it is due to the fact that the contributions to the escape drift term tend to cancel each other when multiple hounds surround the prey. However, when v_e is large compared to the hounds' speed, a strong divergence can occur at vanishing noise intensity in some cases. This divergence relies on specific rare events: i.e. when the hare escapes from the circle of hounds and survives the pursuit for an extremely long time. We understood this phenomenon by comparing the mean and median of the CT, which differ drastically when the mean is dominated by the rare *escape-from-the-circle* events.

The hounds' speed is the value of v_e above which the divergence of the mean CT is possible. For any *finite* ensemble size (see section 4.3), however, the number of hounds N plays a role, whether any *escape-from-the-circle* event, and thus a large increase in the mean CT, is observed. In other words, from the physical point of view, $v_{e,crit}$ is an increasing function of N. In this sense, the interplay between v_e and N plays at weak noise the same role of the interplay between D and N at large noise intensity. In this latter case, the mean CT can grow or decrease as a function of D depending on the number of chasers [51]. Also in this case the growth is caused by trajectories that escape the ring of hounds. Here, however, the *escape-from-the-circle* events are driven by the noise, which is reflected in the different CT distributions as well as the much slower growth with D of the mean CT when $D \to \infty$.

We also showed the distinct effects that a randomization of the initial conditions can have on the capture statistics by adding a vector with random components to the equidistantly distributed hounds over the unit circle. When $v_e \leqslant 1$, we find that the mean CT can be either increased or decreased, or remains almost unchanged—depending on the number of hounds and the range of hare's diffusion coefficient. When $v_e > 1$, the randomized initial conditions tend always to increase the hare's mean survival time by increasing the probability of the *escape-from-the-circle* events.

A consistent finding in all our simulations is that the repulsive escape term always increases the average CT: it is always beneficial—or at least not harmful—for the hare to take the positional information about its

pursuers into account. However, there are many possibilities to make use of this information. In other words, the repulsion term introduced here is certainly only one possible choice, but other sensible evasion strategies are possible. For example, the hare could run away from the closest hound only (a popular choice in pursuit models involving multiple chasers and multiple targets), or a different functional dependence on the distance $g(r)$ could be used in place of an exponential.

Although it seems likely that making (good) use of additional information can only improve the survival chances, the natural domain of application of a stochastic model is a microscopic physical system, and microorganisms can indeed chase nutrients but also have to run away from threats [53, 54]. In this context, predators and preys have to deal with severe uncertainties in sensing each other's position and cannot reliably 'see' each other as in our model [63–66]. Such uncertainties would translate into rotational noise acting on the velocity vector of pursuers and evaders, a kind of noise that can be beneficial or detrimental in the pursuit of a non-random target [8, 47]. It is not clear, however, how this further stochastic element would affect the present model, in particular if the model is endowed with different evasion strategies. As an interesting open question remains whether circumstances exist, in which a repulsion term or evasion strategy can *shorten* the prey's survival time, which would be better off with a purely random motion instead.

Data availability statement

The data that support the findings of this study are available upon reasonable request from the authors.

ORCID iDs

Davide Bernardi https://orcid.org/0000-0002-7043-6606
Benjamin Lindner https://orcid.org/0000-0001-5617-127X

References

[1] Dobbie J M 1975 *SIAM J. Appl. Math.* **28** 72–86
[2] Isaacs R 1999 *Differential Games: a Mathematical Theory With Applications to Warfare and Pursuit, Control and Optimization* (New York: Dover)
[3] Nahin P J 2007 *Chases and Escapes: The Mathematics of Pursuit and Evasion* (Princeton, NJ: Princeton University Press)
[4] Foreman J G 1977 *SIAM J. Control Optim.* **15** 841–56
[5] Mungan C E 2005 *Eur. J. Phys.* **26** 985–90
[6] Weihs D and Webb P 1984 *J. Theor. Biol.* **106** 189–206
[7] Alpern S, Fokkink R, Lindelauf R and Olsder G-J 2008 *SIAM J. Control Optim.* **47** 1178–90
[8] Goh S, Winkler R G and Gompper G 2022 *New J. Phys.* **24** 093039
[9] Nayak I, Nandi A and Das D 2020 *Phys. Rev.* E **102** 062109
[10] de Souza C, Castillo P and Vidolov B 2022 *Robotica* **40** 2697–2715
[11] Scott W and Leonard N E 2013 Pursuit, herding and evasion: a three-agent model of caribou predation *2013 American Control Conf.* pp 2978–83
[12] Schwarzl M, Godec A, Oshanin G and Metzler R 2016 *J. Phys. A: Math. Theor.* **49** 225601
[13] Kamimura A and Ohira T 2010 *New J. Phys.* **12** 053013
[14] Angelani L 2012 *Phys. Rev. Lett.* **109** 118104
[15] Iwama T and Sato M 2012 *Phys. Rev.* E **86** 067102
[16] Lin Y and Abaid N 2013 *Phys. Rev.* E **88** 062724
[17] Yang S, Jiang S, Jiang L, Li G and Han Z 2014 *New J. Phys.* **16** 083006
[18] Saito T, Nakamura T and Ohira T 2016 *Physica* A **447** 172–9
[19] Wang H, Han W and Yang J 2017 *Physica* A **465** 34–39
[20] Janosov M, Virágh C, Vásárhelyi G and Vicsek T 2017 *New J. Phys.* **19** 053003
[21] Surendran A, Plank M and Simpson M 2019 *Sci. Rep.* **9** 14988
[22] Romanczuk P, Couzin I D and Schimansky-Geier L 2009 *Phys. Rev. Lett.* **102** 010602
[23] Šćepanović J R, Karač A, Jakšić Z M, Budinski-Petković L and Vrhovac S B 2019 *Physica* A **525** 450–65
[24] Golestanian R, Liverpool T B and Ajdari A 2005 *Phys. Rev. Lett.* **94** 220801
[25] Sengupta S, Ibele M E and Sen A 2012 *Angew. Chem., Int. Ed. Engl.* **51** 8434–45
[26] Palagi S and Fischer P 2018 *Nat. Rev. Mater.* **3** 113–24
[27] You M, Chen C, Xu L, Mou F and Guan J 2018 *Acc. Chem. Res.* **51** 3006–14
[28] Alvarez L, Fernandez-Rodriguez M, Alegria A, Arrese-Igor S, Zhao K, Kröger M and Isa L 2021 *Nat. Commun.* **12** 4762
[29] Vuijk H D, Merlitz H, Lang M, Sharma A and Sommer J-U 2021 *Phys. Rev. Lett.* **126** 208102
[30] Ghosh P K, Li Y, Marchesoni F and Nori F 2015 *Phys. Rev.* E **92** 012114
[31] Stark H 2018 *Acc. Chem. Res.* **51** 2681–8
[32] Simard F, Desharnais J and Laviolette F 2021 *Theoret. Comput. Sci.* **887** 30–50
[33] Krapivsky P L and Redner S 1996 *J. Phys. A: Math. Gen.* **29** 5347–57
[34] Winkler K and Bray A J 2005 *J. Stat. Mech.: Theory Exp.* **2005** P02005
[35] Gabel A, Majumdar S N, Panduranga N K and Redner S 2012 *J. Stat. Mech.: Theory Exp.* **2012** P05011
[36] Peng J and Agliari E 2019 *Phys. Rev.* E **100** 062310
[37] Weng T, Zhang J, Small M and Hui P 2017 *Europhys. Lett.* **119** 48006
[38] Lomholt M A, Ambjörnsson T and Metzler R 2005 *Phys. Rev. Lett.* **95** 260603

[39] Oshanin G, Wio H S, Lindenberg K and Burlatsky S F 2007 *J. Phys.: Condens. Matter* **19** 065142
[40] Evans M R and Majumdar S N 2011 *Phys. Rev. Lett.* **106** 160601
[41] Mejía-Monasterio C, Oshanin G and Schehr G 2011 *J. Stat. Mech.: Theory Exp.* **2011** P06022
[42] Kusmierz L, Majumdar S N, Sabhapandit S and Schehr G 2014 *Phys. Rev. Lett.* **113** 220602
[43] Palyulin V V, Chechkin A V and Metzler R 2014 *Proc. Natl Acad. Sci.* **111** 2931–6
[44] Pal A and Reuveni S 2017 *Phys. Rev. Lett.* **118** 030603
[45] Falcón-Cortés A, Boyer D, Giuggioli L and Majumdar S N 2017 *Phys. Rev. Lett.* **119** 140603
[46] Jandhyala V K and Fotopoulos S B 2018 *Environmetrics* **29** e2451 e2451 env-16-0136
[47] Noetel J, Freitas V, Macau E and Schimansky-Geier L 2018 *Phys. Rev.* E **98** 022128
[48] Chechkin A and Sokolov I M 2018 *Phys. Rev. Lett.* **121** 050601
[49] Grebenkov D S, Metzler R and Oshanin G 2022 *New J. Phys.* **24** 083035
[50] Oshanin G, Vasilyev O, Krapivsky P L and Klafter J 2009 *Proc. Natl Acad. Sci.* **106** 13696–701
[51] Bernardi D and Lindner B 2022 *Phys. Rev. Lett.* **128** 040601
[52] Schirber M 2022 *Physics* **15** s10
[53] Adler J 1975 *Annu. Rev. Biochem.* **44** 341–56
[54] Webre D J, Wolanin P M and Stock J B 2003 *Curr. Biol.* **13** R47–R49
[55] Gardiner C W 1985 *Handbook of Stochastic Methods* (Berlin: Springer)
[56] Lindner B, Longtin A and Bulsara A 2003 *Neural Comput.* **15** 1761–88
[57] Schrödinger E 1915 *Phys.* Z. **16** 289–95
[58] Kramers H A 1940 *Physica* **7** 284
[59] Risken H 1996 Fokker-Planck equation *The Fokker-Planck Equation* (Berlin: Springer)
[60] Hänggi P, Talkner P and Borkovec M 1990 *Rev. Mod. Phys.* **62** 251–341
[61] Ricciardi L M 1977 The first passage time problem *Diffusion Processes and Related Topics in Biology* (Berlin: Springer)
[62] Lindner B 2002 *Coherence and Stochastic Resonance in Nonlinear Dynamical Systems* (Berlin: Logos-Verlag)
[63] Tostevin F and ten Wolde P R 2009 *Phys. Rev. Lett.* **102** 218101
[64] Tkačik G and Bialek W 2016 *Annu. Rev. Condens. Matter Phys.* **7** 89–117
[65] Barberis L and Peruani F 2016 *Phys. Rev. Lett.* **117** 248001
[66] Mattingly H H, Kamino K, Machta B B and Emonet T 2021 *Nat. Phys.* **17** 1426–31